

$\Xi(1690)$ as a $\bar{K}\Sigma$ molecular state

Takayasu Sekihara

Research Center for Nuclear Physics (RCNP), Osaka University, Ibaraki, Osaka, 567-0047, Japan

.....
We show that a Ξ^* pole can be dynamically generated near the $\bar{K}\Sigma$ threshold as an s -wave $\bar{K}\Sigma$ molecular state in a coupled-channels unitary approach with the leading-order chiral interaction. This Ξ^* state can be identified with the $\Xi(1690)$ resonance with $J^P = 1/2^-$. We find that the experimental $\bar{K}^0\Lambda$ and $K^-\Sigma^+$ mass spectra are qualitatively reproduced with the Ξ^* state. Moreover we theoretically investigate properties of the dynamically generated Ξ^* state.

1. Introduction Investigating the internal structure of hadrons is one of the most important subjects in hadron physics. The motivation for the investigation is that we expect the existence of exotic hadrons, which are not able to be classified as qqq for baryons nor $q\bar{q}$ for mesons. Actually, the fundamental theory of strong interaction, QCD, does not prohibit such exotic systems as long as they are color singlet, and there are indeed several exotic hadron candidates which cannot fit into the classifications by the constituent quark models [1]. In order to clarify the internal structure of exotic hadron candidates and to discover genuine exotic hadrons, great efforts have been continuously made in both experimental and theoretical sides. In this context, it is very encouraging that charged quarkonium-like states and charmonium-pentaquark states were observed in the heavy quark sector by Belle [2] and by LHCb [3], respectively.

In this Article we focus on the $\Xi(1690)$ resonance and theoretically investigate its structure in terms of the $\bar{K}\Sigma$ component. Historically this resonance was discovered as a threshold enhancement in both the neutral and charged $\bar{K}\Sigma$ mass spectra in the $K^-p \rightarrow (\bar{K}\Sigma)K\pi$ reaction at 4.2 GeV/c [4]. Several experimental and theoretical studies have followed in, *e.g.*, Refs. [5–11] and Refs. [12–20], respectively, and today the $\Xi(1690)$ resonance is attributed a three-star status in the Particle Data Group table [1]. Its mass and width are 1690 ± 10 MeV and < 30 MeV, respectively [1], but a relatively narrow width, *e.g.*, 10 ± 6 MeV [7] was reported as well. In addition, the small ratio of the $\Xi(1690)$ branching fractions $\Gamma(\pi\Xi)/\Gamma(\bar{K}\Sigma) < 0.09$ has been observed [1]. Its spin/parity has been expected to be $J^P = 1/2^-$ from the beginning [4], and this was supported by a recent experiment [10]. Then, a difficulty emerges; assuming $J^P = 1/2^-$, $\Xi(1690)$ couples to the $\pi\Xi$ channel in s wave, and hence $\Xi(1690)$, as a qqq state, should inevitably decay to the $\pi\Xi$ channel to some extent in a naïve quark model, which contradicts the above experimental results and implications. This implies that $\Xi(1690)$ might have some nontrivial structure than usual qqq state.

In this study, in order to describe $\Xi(1690)$, we perform a coupled-channel analysis of the s -wave $\bar{K}\Sigma$, $\bar{K}\Lambda$, $\pi\Xi$, and $\eta\Xi$ scatterings. For this purpose we employ the so-called chiral unitary approach [21–25], which is formulated with the meson–baryon coupled-channels scattering equation in an algebraic form based on the combination of the chiral perturbation theory and the unitarization of the scattering amplitude. One of the most remarkable properties of this approach is that a simple driving term, or interaction kernel, provided by the chiral Lagrangian with a small number of free parameters can reproduce experimental observables such as cross sections fairly well. The

most important application of the chiral unitary approach is the description of the $\Lambda(1405)$ resonance [26]. In this Article we apply the chiral unitary approach to the strangeness $S = -2$ sector, where Ξ^* resonances exist. In the chiral unitary approach the $S = -2$ sector was already studied in Refs. [15, 18, 27]. On the one hand, in Ref. [27] a Ξ^* state below the $\bar{K}\Lambda$ threshold was discussed and identified with $\Xi(1620)$. On the other hand, in Refs. [15, 18] the authors obtained several Ξ^* poles such as $\Xi(1620)$, $\Xi(1690)$, and $\Xi(1950)$ together with many hadronic resonances in $S = 0$ to -3 . Especially in Ref. [15] they found that in a flavor $SU(3)$ symmetric world $\Xi(1690)$ is a member of two degenerated octets, which also contain one of the two- $\Lambda(1405)$ poles coming from the $\bar{K}N$ bound state, $N(1535)$, and so on. In this study we extend the analyses in Refs. [15, 27] by concentrating on the phenomena near the $\bar{K}\Sigma$ threshold and on $\Xi(1690)$. In the following we will show that the chiral unitary approach in $S = -2$ can qualitatively reproduce the experimental data of the $\bar{K}^0\Lambda$ and $K^-\Sigma^+$ mass spectra, dynamically generate a $\Xi(1690)$ pole as an s -wave $\bar{K}\Sigma$ molecular state near the $\bar{K}\Sigma$ threshold, and naturally explain the decay properties of $\Xi(1690)$.

2. Formulation First of all we formulate the meson–baryon scattering amplitude $T_{jk}(w)$ in s wave in the chiral unitary approach, where w is the center-of-mass energy and j and k are the channel indices. The scattering amplitude is the solution of the Bethe–Salpeter equation in a coupled-channels algebraic form

$$T_{jk}(w) = V_{jk}(w) + \sum_l V_{jl}(w)G_l(w)T_{lk}(w), \quad (1)$$

with the interaction kernel V_{jk} taken from the chiral perturbation theory and the meson–baryon loop function G_j . The treatment of the algebraic form was justified first by the so-called on-shell factorization [22] and then by the dispersion relation and the N/D method [23]. In this study we consider the system with $S = -2$ and charge $Q = 0$ or -1 , where we take into account six two-body channels ($K^-\Sigma^+$, $\bar{K}^0\Sigma^0$, $\bar{K}^0\Lambda$, $\pi^+\Xi^-$, $\pi^0\Xi^0$, and $\eta\Xi^0$) for the neutral states and similarly six channels ($\bar{K}^0\Sigma^-$, $K^-\Sigma^0$, $K^-\Lambda$, $\pi^-\Xi^0$, $\pi^0\Xi^-$, and $\eta\Xi^-$) for the charged states. These channels are labeled by the indices $j = 1, \dots, 6$ in the above orders for the neutral and charged states, respectively. For the interaction kernel V_{jk} we use the leading-order chiral perturbation theory in s wave, i.e., the Weinberg–Tomozawa interaction. After the projection to the s wave, the interaction is expressed as

$$V_{jk}(w) = -\frac{C_{jk}}{4f_j f_k}(2w - M_j - M_k)\sqrt{\frac{E_j + M_j}{2M_j}}\sqrt{\frac{E_k + M_k}{2M_k}}, \quad (2)$$

with the j th channel meson decay constant f_j , baryon energy $E_j \equiv (s + M_j^2 - m_j^2)/(2w)$, the squared center-of-mass energy $s \equiv w^2$, and the baryon and meson masses M_j and m_j in the j th channel, respectively. In this study we use the physical masses unless explicitly mentioned. The factor C_{jk} is the Clebsch–Gordan coefficient determined from the group structure of the flavor $SU(3)$ symmetry and its value is listed in Table 1. The meson decay constants are chosen at their physical values [1]: $f_\pi = 92.2$ MeV, $f_K = 1.2f_\pi$, and $f_\eta = 1.3f_\pi$. Since V_{jk} in Eq. (2) depends only on the center-of-mass energy w , we can put V_{jk} out of the loop integral in the scattering equation, which hence becomes an algebraic form in Eq. (1). For the meson–baryon loop function $G_j(w)$, we take a covariant expression and calculate the integral with the dimensional regularization. As a result, the loop function depends on a subtraction constant $a_j(\mu_{\text{reg}})$ in each channel at the regularization scale μ_{reg} . The explicit expression of the loop function can be found in Ref. [28]. An important point to be noted is that the interaction kernel does not contain free parameters at the present order and its

Table 1 Coefficients $C_{jk} = C_{kj}$ for the channels in $Q = 0$ and $S = -2$. From these values we can obtain the coefficients for the channels in $Q = -1$ and $S = -2$ by using the relation $C_{jk}(Q = -1, S = -2) = \xi_j \xi_k C_{jk}(Q = 0, S = -2)$ with $\xi_1 = \xi_3 = \xi_4 = \xi_6 = +1$ and $\xi_2 = \xi_5 = -1$.

	$K^-\Sigma^+$	$\bar{K}^0\Sigma^0$	$\bar{K}^0\Lambda$	$\pi^+\Xi^-$	$\pi^0\Xi^0$	$\eta\Xi^0$
$K^-\Sigma^+$	1	$-\sqrt{2}$	0	0	$-1/\sqrt{2}$	$-\sqrt{3/2}$
$\bar{K}^0\Sigma^0$	$-\sqrt{2}$	0	0	$-1/\sqrt{2}$	$-1/2$	$\sqrt{3/4}$
$\bar{K}^0\Lambda$	0	0	0	$-\sqrt{3/2}$	$\sqrt{3/4}$	$-3/2$
$\pi^+\Xi^-$	0	$-1/\sqrt{2}$	$-\sqrt{3/2}$	1	$-\sqrt{2}$	0
$\pi^0\Xi^0$	$-1/\sqrt{2}$	$-1/2$	$\sqrt{3/4}$	$-\sqrt{2}$	0	0
$\eta\Xi^0$	$-\sqrt{3/2}$	$\sqrt{3/4}$	$-3/2$	0	0	0

strength is fixed entirely by the coefficients C_{jk} and the meson decay constants. Therefore, only the subtraction constant in each channel is the model parameter. In this study we assume the isospin symmetry for the subtraction constants, *e.g.*, $a_{\bar{K}\Sigma} = a_{K^-\Sigma^+} = a_{\bar{K}^0\Sigma^0}$, so we will have four model parameters in neutral and charged $S = -2$ systems, respectively.

When the interaction is enough attractive, the interaction can dynamically generate a pole of the scattering amplitude for a resonance or a bound state. The pole is characterized by the pole position w_{pole} and its residue $g_j g_k$:

$$T_{jk}(w) = \frac{g_j g_k}{w - w_{\text{pole}}} + (\text{regular at } w = w_{\text{pole}}). \quad (3)$$

The constant g_j can be interpreted as the coupling constant of the resonance to the j th two-body channel. The pole position and residue reflect the structure of the resonance. Recently this statement is formulated in terms of the compositeness [29, 30]. First it was shown in Refs. [31, 32] that the j th channel two-body wave function is proportional to the coupling constant g_j for an energy independent separable interaction, and then the case of a general separable interaction, including the present formulation, was studied in Ref. [33]. In the present formulation, we can calculate the j th channel two-body wave function for the resonance as [33]

$$\tilde{\Psi}_j(\mathbf{q}) = \frac{g_j \sqrt{4M_j w_{\text{pole}}}}{w_{\text{pole}}^2 - [\omega_j(\mathbf{q}) + \Omega_j(\mathbf{q})]^2}, \quad \omega_j(\mathbf{q}) \equiv \sqrt{m_j^2 + \mathbf{q}^2}, \quad \Omega_j(\mathbf{q}) \equiv \sqrt{M_j^2 + \mathbf{q}^2}, \quad (4)$$

with the relative momentum of the state \mathbf{q} , and the j th channel compositeness X_j is obtained as the norm of the j th channel two-body wave function as [33]

$$X_j \equiv \int \mathcal{D}\mathbf{q} \left[\tilde{\Psi}_j(\mathbf{q}) \right]^2 = -g_j^2 \left[\frac{dG_j}{dw} \right]_{w=w_{\text{pole}}}, \quad \mathcal{D}\mathbf{q} \equiv \frac{d^3q}{(2\pi)^3} \frac{\omega_j(\mathbf{q}) + \Omega_j(\mathbf{q})}{2\omega_j(\mathbf{q})\Omega_j(\mathbf{q})}. \quad (5)$$

where the measure $\mathcal{D}\mathbf{q}$ guarantees the Lorentz invariance of the integral and we have transformed the integral into the derivative of the loop function (for details of the calculation, see Ref. [33]). Here we note that we do not calculate the absolute value squared but the complex number squared of $\tilde{\Psi}_j(\mathbf{q})$ since we employ the Gamow vector for the resonance so as to obtain the correct normalization of the resonance wave function [33]. In addition to the compositeness, one can calculate the elementariness Z as the contributions from implicit channels, which do not appear as explicit degrees of freedom in the practical model space, such as compact qqq states. Namely, on the assumption that the energy

dependence of the interaction originates from implicit channels, the elementariness is expressed as [33]

$$Z = - \sum_{j,k} g_k g_j \left[G_j \frac{dV_{jk}}{dw} G_k \right]_{w=w_{\text{pole}}} . \quad (6)$$

Then it is important that the sum of the compositeness and elementariness coincides with the normalization of the total wave function for the resonance $|\Psi\rangle$ and is exactly unity [33]:

$$\langle \Psi^* | \Psi \rangle = \sum_j X_j + Z = 1, \quad (7)$$

where the bra state $\langle \Psi^* |$ has been used to correctly normalize the resonance wave function in terms of the Gamow vector. The condition of the correct normalization as unity (7) is guaranteed by a generalized Ward identity proved in Ref. [28]. We note that in general both the compositeness X_j and elementariness Z are not observable and hence are model dependent quantities. Furthermore, they become complex for a resonance state, so we cannot interpret the compositeness (elementariness) as the probability of finding a two-body (implicit) component inside the resonance. However, based on the normalization (7), we can interpret it for a resonance with a wave function similar to a bound state one, as for the Ξ^* resonance in the following discussions.

3. Numerical results Now we solve the scattering equation to obtain the scattering amplitude $T_{jk}(w)$ and show the numerical results. In the following we mainly consider the neutral charge system since the experimental data on both the $\bar{K}^0\Lambda$ and $K^-\Sigma^+$ mass spectra are available [8].

As we have explained, we have four subtraction constants as the model parameters. First we fix them by using the so-called natural renormalization scheme [34], which can exclude explicit pole contributions from the loop functions. In the natural renormalization scheme, we introduce a certain energy w_m at which we achieve the consistency of the low-energy theorem with respect to the spontaneous breaking of the chiral symmetry. Namely, since we take the interaction V as the leading order term of the chiral perturbation theory, we require that the scattering amplitude T should coincide with the interaction V at certain “low” energy according to the low-energy theorem. We represent this energy as w_m : $T_{jk}(w_m) = V_{jk}(w_m)$ with $G_j(w_m) = 0$ in every channel j . According to the discussion in Ref. [34], we fix this matching energy scale as the mass of the “target” baryon of the scatterings, i.e., $w_m = M_\Lambda$, M_Σ , or M_Ξ .¹ As a result, we obtain the subtraction constants in the second, third, and fourth columns of Table 2, to which we refer as the parameter sets Λ , Σ , and Ξ , respectively.² With the parameter set Λ , we find two resonance poles as Ξ^* states with $J^P = 1/2^-$; each pole is in the second (unphysical) Riemann sheets of the open channels, whose thresholds are lower than $\text{Re}(w_{\text{pole}})$. One pole is located at $1556.5 - 102.9i$ MeV, which corresponds to the pole studied in Ref. [15, 18, 27] as the $\Xi(1620)$ resonance. We have found that the energy dependence of the Weinberg–Tomozawa interaction in the $\pi\Xi$ channel is essential to the appearance of $\Xi(1620)$. Actually, by taking into account only the $\pi\Xi$ channel and switching off couplings to other channels, we obtain a resonance pole at a similar position in the $\pi\Xi$ dynamics. The mechanism is the same as that of the broad $\Lambda(1405)$ pole in the chiral unitary approach, to which the energy dependence

¹ We note that the energy $w_m = M_\Lambda$ is on the left-hand cut of the $\pi\Xi$ channel. Nevertheless, we employ this energy as the matching scale, since the $\pi\Xi$ contribution to $\Xi(1690)$ is found negligible.

² Since we assume the isospin symmetry for the subtraction constants, these subtraction constants are obtained with isospin symmetric masses for hadrons in the natural renormalization scheme.

Table 2 Parameter sets Λ , Σ , Ξ , and Fit, and properties of the neutral $\Xi(1690)$ state. The regularization scale is $\mu_{\text{reg}} = 630$ MeV in all channels. We also show the χ^2 value for the $\bar{K}^0\Lambda$ and $K^-\Sigma^+$ mass spectra divided by the number of degrees of freedom, $\chi^2/N_{\text{d.o.f.}}$, and the ratio of the two branching fractions R defined in Eq. (11).

	Set Λ	Set Σ	Set Ξ	Fit
$a_{\bar{K}\Sigma}$	-2.30	-2.23	-2.10	-1.98
$a_{\bar{K}\Lambda}$	-2.15	-2.07	-1.91	-2.07
$a_{\pi\Xi}$	-2.08	-1.99	-1.77	-0.75
$a_{\eta\Xi}$	-2.57	-2.52	-2.43	-3.31
$\chi^2/N_{\text{d.o.f.}}$	65.3/57	66.6/57	81.2/57	59.0/57
R	1.32	3.04	6.07	1.06
w_{pole}	1682.6 - 0.8 <i>i</i> MeV			1684.3 - 0.5 <i>i</i> MeV
$g_{K^-\Sigma^+}$	1.00 + 0.22 <i>i</i>	No $\Xi(1690)$ pole	No $\Xi(1690)$ pole	1.02 + 0.60 <i>i</i>
$g_{\bar{K}^0\Sigma^0}$	-0.73 - 0.15 <i>i</i>			-0.76 - 0.41 <i>i</i>
$g_{\bar{K}^0\Lambda}$	0.24 - 0.04 <i>i</i>			0.38 + 0.20 <i>i</i>
$g_{\pi^+\Xi^-}$	0.04 + 0.08 <i>i</i>			0.06 - 0.05 <i>i</i>
$g_{\pi^0\Xi^0}$	-0.05 - 0.05 <i>i</i>			-0.09 + 0.05 <i>i</i>
$g_{\eta\Xi^0}$	-0.76 - 0.17 <i>i</i>			-0.66 - 0.48 <i>i</i>
$X_{K^-\Sigma^+}$	0.77 - 0.10 <i>i</i>			0.83 - 0.31 <i>i</i>
$X_{\bar{K}^0\Sigma^0}$	0.12 + 0.04 <i>i</i>			0.12 + 0.17 <i>i</i>
$X_{\bar{K}^0\Lambda}$	0.00 + 0.00 <i>i</i>			-0.02 + 0.00 <i>i</i>
$X_{\pi^+\Xi^-}$	0.00 + 0.00 <i>i</i>			0.00 + 0.00 <i>i</i>
$X_{\pi^0\Xi^0}$	0.00 + 0.00 <i>i</i>			0.00 + 0.00 <i>i</i>
$X_{\eta\Xi^0}$	0.02 + 0.01 <i>i</i>			0.01 + 0.02 <i>i</i>
Z	0.08 + 0.04 <i>i</i>			0.06 + 0.11 <i>i</i>

of the Weinberg–Tomozawa interaction in the $\pi\Sigma$ channel is essential. In addition to the $\Xi(1620)$ pole, another pole appears at 1682.6 - 0.8i MeV just below the $\bar{K}\Sigma$ threshold, whose properties are listed in the second column of Table 2. We expect that the latter pole can be identified with the $\Xi(1690)$ resonance and originates from the $\bar{K}\Sigma$ bound state. On the other hand, with the parameter sets Σ and Ξ , we obtain no poles near the $\bar{K}\Sigma$ threshold as $\Xi(1690)$. However, we will not take these parameter sets seriously, since they give larger value of the ratio R with larger χ^2 value introduced below and can be excluded by the experimental results.

Let us now concentrate on the Ξ^* state near the $\bar{K}\Sigma$ threshold in the parameter set Λ . The structure of the Ξ^* state can be investigated with the coupling constants and compositeness. Actually, from Table 2 the coupling constants and compositeness indicate a large $\bar{K}\Sigma$ component in the Ξ^* state. Especially the $\bar{K}\Sigma$ compositeness, $X_{K^-\Sigma^+} + X_{\bar{K}^0\Sigma^0}$, dominates the sum rule (7) with its small imaginary part. This result strongly indicates that the Ξ^* state is indeed a $\bar{K}\Sigma$ molecular state, on the basis of the similarity to the bound state case; the wave function of the Ξ^* state can be similar to that of a bound state dominated by the $\bar{K}\Sigma$ channel. We also note that, although the coupling constant approximately satisfies the isospin relation $g_{K^-\Sigma^+} = -\sqrt{2}g_{\bar{K}^0\Sigma^0}$, the $\bar{K}\Sigma$ compositeness largely breaks the corresponding relation $X_{K^-\Sigma^+} = 2X_{\bar{K}^0\Sigma^0}$. This is because the Ξ^* state is located very

close to the $K^-\Sigma^+$ threshold. This fact will induce further effects of the isospin symmetry breaking on $\Xi(1690)$, such as the difference of the $K^-\Sigma^+$ and $\bar{K}^0\Sigma^0$ mass spectra, due to the difference of their thresholds. The dominance of the $K^-\Sigma^+$ compositeness implies a coupled-channels extension of the near-threshold scaling in s wave discussed in Refs. [35, 36].

In addition to the $\bar{K}\Sigma$ component, the Ξ^* state has a remarkable property of its small decay width with the small imaginary part of the pole position ~ 1 MeV, which can be seen also in Refs. [15, 18]. This decay property can be understood by considering the structure of the coefficient C_{jk} . Namely, as shown in Table 1, the transitions $K^-\Sigma^+$, $\bar{K}^0\Sigma^0 \leftrightarrow \bar{K}^0\Lambda$ are forbidden at the leading order, so the decay of the $\bar{K}\Sigma$ quasibound state to the $\bar{K}\Lambda$ channel is highly suppressed. Actually, the decay to $\bar{K}\Lambda$ takes place through a multiple scattering of $\bar{K}\Sigma \rightarrow \eta\Xi \rightarrow \bar{K}\Lambda$, since the $\bar{K}\Sigma$ - $\eta\Xi$ coupling is the strongest among the coupled channels [27]. In addition, the $\bar{K}\Sigma \leftrightarrow \pi\Xi$ transition is not strong compared to, *e.g.*, the $\bar{K}N \leftrightarrow \pi\Sigma$ one in the $\Lambda(1405)$ case; the coefficient $C_{\bar{K}\Sigma\pi\Xi(I=1/2)}$ in the isospin basis is $-1/2$ [27], while that of $\bar{K}N \leftrightarrow \pi\Sigma$ in $I = 0$ is $-\sqrt{3/2}$ [22]. As a consequence, the Ξ^* state as a $\bar{K}\Sigma$ molecule cannot couple strongly to $\bar{K}\Lambda$ nor $\pi\Xi$ as the decay channels and hence the decay width becomes very small. Moreover, the above argument can also explain the small ratio of the $\Xi(1690)$ branching fractions $\Gamma(\pi\Xi)/\Gamma(\bar{K}\Sigma) < 0.09$ [1]. Here we note that higher-order contributions to the interaction, such as the s - and u -channel Born terms, can bring tree-level couplings of $\bar{K}\Sigma \leftrightarrow \bar{K}\Lambda$ and may give a decay width $\lesssim 10$ MeV.

Next, in order to make things more accurate, we fit the $\bar{K}^0\Lambda$ and $K^-\Sigma^+$ mass spectra to the experimental data taken from the decay processes $\Lambda_c^+ \rightarrow \Xi(1690)^0 K^+ \rightarrow (\bar{K}^0\Lambda)K^+$ and $(K^-\Sigma^+)K^+$ in Ref. [8]. The scale of two mass spectra is fixed with the central values of $\mathcal{B}[\Lambda_c^+ \rightarrow \Xi(1690)^0 K^+ \rightarrow (\bar{K}^0\Lambda)K^+] = (1.3 \pm 0.5) \times 10^{-3}$ and $\mathcal{B}[\Lambda_c^+ \rightarrow \Xi(1690)^0 K^+ \rightarrow (K^-\Sigma^+)K^+] = (8.1 \pm 3.0) \times 10^{-4}$ [1], respectively. In this study, according to Ref. [37], we calculate the two mass spectra with the correct phase-space factor and a constant prefactor C as

$$\frac{d\Gamma_{(\bar{K}^0\Lambda)K^+}}{dM_{\bar{K}^0\Lambda}} = C p_K p_\Lambda^* |T_{\bar{K}\Sigma(I=1/2) \rightarrow \bar{K}^0\Lambda}|^2, \quad \frac{d\Gamma_{(K^-\Sigma^+)K^+}}{dM_{K^-\Sigma^+}} = C p_K p_\Sigma^* |T_{\bar{K}\Sigma(I=1/2) \rightarrow K^-\Sigma^+}|^2, \quad (8)$$

where $M_{\bar{K}Y}$ is the invariant mass of the $\bar{K}Y = \bar{K}^0\Lambda$ or $K^-\Sigma^+$ system and p_K (p_Y^*) is the momentum of K^+ (hyperon Y) in the Λ_c^+ ($\bar{K}Y$) rest frame. The constant C is common to the two modes, since we expect that both the two mass spectra are obtained with the decay of $\Xi(1690)$ as a $\bar{K}\Sigma(I = 1/2)$ molecular state, and C is determined by the fitting procedure together with the subtraction constants. Moreover, the scattering amplitude $\bar{K}\Sigma(I = 1/2) \rightarrow j$ [$j = 1$ ($K^-\Sigma^+$), 3 ($\bar{K}^0\Lambda$)] is calculated as

$$T_{\bar{K}\Sigma(I=1/2) \rightarrow j} = -\sqrt{\frac{2}{3}}T_{1j} + \sqrt{\frac{1}{3}}T_{2j}, \quad (9)$$

where we have used the $\bar{K}\Sigma(I = 1/2)$ state in our convention

$$|\bar{K}\Sigma(I = 1/2, I_z = 1/2)\rangle = -\sqrt{\frac{2}{3}}|K^-\Sigma^+\rangle + \sqrt{\frac{1}{3}}|\bar{K}^0\Sigma^0\rangle. \quad (10)$$

From the best fit to the $\bar{K}^0\Lambda$ and $K^-\Sigma^+$ mass spectra shown in Fig. 1, we obtain the subtraction constants in the fifth column of Table 2 (Fit). With the parameter set Fit, a Ξ^* state is dynamically generated as a pole at $1684.3 - 0.5i$ MeV as in Table 2. Since this Ξ^* pole qualitatively reproduces the $\Xi(1690)$ peak in the mass spectra as shown in Fig. 1, we can identify this Ξ^* state with the $\Xi(1690)$ resonance.

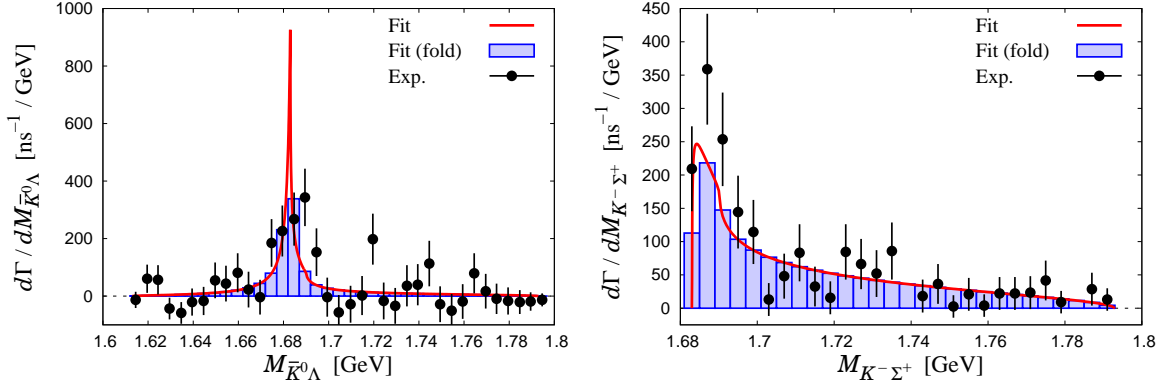


Fig. 1 Mass spectra of $\bar{K}^0\Lambda$ (left) and $K^-\Sigma^+$ (right) calculated with Eq. (8). The red solid lines are the theoretical mass spectra with the fitted parameters and $C = 0.222 \text{ ns}^{-1}/\text{GeV}$, and the blue histograms correspond to the folded results with the size of experimental bins, 5 MeV and 4 MeV for $\bar{K}^0\Lambda$ and $K^-\Sigma^+$, respectively. Experimental data are taken from Ref. [8], and their scale is fixed with the experimental branching fractions (see text).

An important point for the mass spectra in Fig. 1 is that, although we employ the simplest interaction, i.e., the Weinberg–Tomozawa interaction, our scattering amplitude qualitatively reproduces the experimental $\Xi(1690)^0$ peaks in both the $\bar{K}^0\Lambda$ and $K^-\Sigma^+$ mass spectra. Especially we emphasize that the $K^-\Sigma^+$ mass spectrum shows a rapid enhancement at its threshold, which is a consequence of the fact that there is $\Xi(1690)$ near the $K^-\Sigma^+$ threshold. The peak height of the enhancement reflects how strong $\Xi(1690)$ couples to the $K^-\Sigma^+$ channel, or in other words how much $\Xi(1690)$ contains the $K^-\Sigma^+$ component. In this sense, it is essential to observe both the $\bar{K}\Sigma$ and $\bar{K}^0\Lambda$ mass spectra and to determine the relative strength between them in experiments. The enhancement of the $K^-\Sigma^+$ mass spectrum can be evaluated with the ratio of the two branching fractions as

$$R \equiv \frac{\mathcal{B}[\Lambda_c^+ \rightarrow \Xi(1690)^0 K^+ \rightarrow (K^-\Sigma^+) K^+]}{\mathcal{B}[\Lambda_c^+ \rightarrow \Xi(1690)^0 K^+ \rightarrow (\bar{K}^0\Lambda) K^+]}, \quad (11)$$

whose experimental value is $[(8.1 \pm 3.0) \times 10^{-4}]/[(1.3 \pm 0.5) \times 10^{-3}] = 0.62 \pm 0.33$ [1]. Theoretically R is obtained by the ratio of integrals of the two mass spectra, and the result is shown in Table 2. The theoretical values of R overestimate the experimental one, and especially the parameter sets Σ and Ξ can be excluded. On the other hand, the R value of the set Fit is in 2σ errors of the experimental value, although the statistical error is not small for the experimental value. Therefore, an experimental determination of R can constrain more the $\bar{K}\Sigma$ scattering amplitude and the structure of the $\Xi(1690)$ resonance.

We note that the $\Xi(1690)$ pole in the parameter set Fit is located in the first Riemann sheet of the $K^-\Sigma^+$, $\bar{K}^0\Sigma^0$, and $\eta\Xi^0$ channels and in the second Riemann sheet of the $\bar{K}^0\Lambda$, $\pi^+\Xi^-$, and $\pi^0\Xi^0$ channels. Therefore, this pole exists above the $K^-\Sigma^+$ threshold (1683.05 MeV) but in the first Riemann sheet of this channel, which is connected smoothly from the pole position of parameter set Λ . In this meaning, strictly speaking, the peak seen in the $\bar{K}^0\Lambda$ mass spectrum in Fig. 1 is a cusp at the $K^-\Sigma^+$ threshold rather than the usual Breit–Wigner resonance peak. Other properties of $\Xi(1690)$ in the parameter set Fit are very similar to those in the parameter set Λ . The $\pi\Xi$ subtraction constant in the set Fit is larger than “natural” value ~ -2 [23], but we do not take it seriously

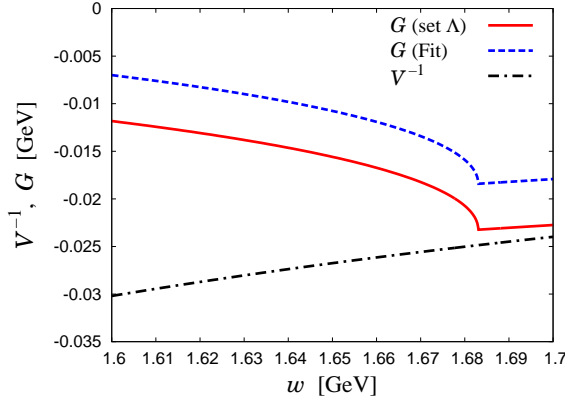


Fig. 2 Loop function G in the $K^-\Sigma^+$ channel and inverse of the interaction V in the $\bar{K}\Sigma(I=1/2)$ channel [see Eq. (12)]. The $K^-\Sigma^+$ threshold is located at 1683.05 MeV.

since the $\pi\Xi$ channel negligibly contribute to the $\Xi(1690)$ resonance. Actually, even changing the subtraction constant $a_{\pi\Xi} = -0.75$ to -2 in the set Fit, we obtain a similar χ^2 value.

4. *Discussion* Next we investigate the origin of the $\Xi(1690)$ pole in our scattering amplitude. First we expect that, from the value of the $\bar{K}\Sigma$ compositeness, the Ξ^* state originates from a $\bar{K}\Sigma$ bound state. In order to check this, we clarify whether the chiral $\bar{K}\Sigma$ interaction in the isospin $I = 1/2$ is attractive enough to generate a bound state when the couplings to other channels are switched off. By using the $\bar{K}\Sigma$ state in the isospin basis in Eq. (10), the $\bar{K}\Sigma$ interaction in $I = 1/2$ is expressed as

$$V_{\bar{K}\Sigma(I=1/2)} = \frac{2}{3}V_{11} - \frac{\sqrt{2}}{3}(V_{12} + V_{21}) + \frac{1}{3}V_{22}. \quad (12)$$

In case of a single channel problem, a bound state appears at the energy which satisfies $V^{-1} = G$ below the threshold. Therefore, we compare the behavior of the loop function G in the $K^-\Sigma^+$ channel and the inverse of the $\bar{K}\Sigma(I=1/2)$ interaction $[V_{\bar{K}\Sigma(I=1/2)}]^{-1}$, which are plotted in Fig. 2. A bound state would appear at the energy where the lines G and V^{-1} intersect each other in Fig. 2, but in fact there is no intersection as the inverse of the interaction V^{-1} is a bit below the loop function G . This means that the chiral $\bar{K}\Sigma$ interaction is attractive but not enough to generate a bound state in a single channel problem. This is in contrast to the $\bar{K}N(I=0)$ interaction, which can solely generate a bound state as the origin of the $\Lambda(1405)$ resonance [38]. In addition, this fact implies that the multiple scatterings such as $\bar{K}\Sigma \rightarrow \eta\Xi \rightarrow \bar{K}\Sigma$ assist the $\bar{K}\Sigma$ interaction in dynamically generating a $\bar{K}\Sigma$ quasibound state which is located very close to the $\bar{K}\Sigma$ threshold. In the multiple scatterings the $\eta\Xi$ channel will be the most important, since the coefficient C_{jk} of the $\bar{K}\Sigma$ - $\eta\Xi$ coupling is the strongest among the coupled channels. This can be seen also from the large coupling constant $g_{\eta\Xi}$ in Table 2, which is comparable to the $\bar{K}\Sigma$ coupling constants. Here we note that, when the kaon decay constant is chosen to be $f_K = f_\pi \approx 90$ MeV, attraction of the $\bar{K}\Sigma$ interaction will become stronger and the $\bar{K}\Sigma$ interaction may be able to solely generate a bound state. As a result, in this condition the binding energy of the $\bar{K}\Sigma$ system as $\Xi(1690)$ will be several tens of MeV, which was indeed achieved in Ref. [15]. Furthermore, the subtraction constant $a_{\eta\Xi}$ is negatively large compared to the values in the natural renormalization scheme. This would reflect effects from implicit channels such as $\bar{K}^*\Sigma$, which were taken into account in Ref. [18].

Finally we consider the charged $S = -2$ system with the channels $\bar{K}^0\Sigma^-$, $K^-\Sigma^0$, $K^-\Lambda$, $\pi^-\Xi^0$, $\pi^0\Xi^-$, and $\eta\Xi^-$. Here we use the parameter set Fit given in Table 2 for the subtraction constants and solve the Bethe–Salpeter equation (1) to obtain the scattering amplitude. As a result, with the set Fit

Table 3 Properties of the charged $\Xi(1690)$ state with the parameter set “Fit” for the neutral $\Xi(1690)$ state. The pole position is $w_{\text{pole}} = 1693.4 - 10.5i$ MeV.

Fit			
$g_{\bar{K}^0\Sigma^-}$	$2.17 + 0.29i$	$X_{\bar{K}^0\Sigma^-}$	$0.86 - 0.50i$
$g_{K^-\Sigma^0}$	$1.36 + 0.07i$	$X_{K^-\Sigma^0}$	$-0.27 + 0.31i$
$g_{K^-\Lambda}$	$0.76 + 0.04i$	$X_{K^-\Lambda}$	$-0.02 + 0.04i$
$g_{\pi^-\Xi^0}$	$0.18 - 0.09i$	$X_{\pi^-\Xi^0}$	$0.00 + 0.00i$
$g_{\pi^0\Xi^-}$	$-0.07 - 0.20i$	$X_{\pi^0\Xi^-}$	$0.00 + 0.00i$
$g_{\eta\Xi^-}$	$-1.41 - 0.33i$	$X_{\eta\Xi^-}$	$0.07 + 0.03i$
		Z	$0.36 + 0.12i$

we find a pole near the $\bar{K}\Sigma$ threshold, which corresponds to the $\Xi(1690)^-$ resonance. The pole is located in the first Riemann sheet of the $\bar{K}^0\Sigma^-$ and $\eta\Xi^-$ channels and in the second Riemann sheet of the $K^-\Lambda$, $K^-\Sigma^0$, $\pi^-\Xi^0$, and $\pi^0\Xi^-$ channels. The properties of $\Xi(1690)^-$ are listed in Table 3. The pole position has a larger imaginary part ~ 10 MeV compared to the neutral case, since it exists above the $K^-\Sigma^0$ threshold in its second Riemann sheet and hence the decay $\Xi(1690)^- \rightarrow K^-\Sigma^0$ is allowed. The coupling constants and compositeness indicate that $\Xi(1690)^-$ has a large $\bar{K}\Sigma$ component. However, each of $\bar{K}^0\Sigma^-$ and $K^-\Sigma^0$ compositeness has a nonnegligible imaginary part, because the pole exists above the $K^-\Sigma^0$ one in its second Riemann sheet. Nevertheless, the sum $X_{\bar{K}^0\Sigma^-} + X_{K^-\Sigma^0}$ is the largest contribution to the sum rule (7) with its small imaginary part, which implies that the charged Ξ^* state is also a $\bar{K}\Sigma$ molecular state. Moreover, we can expect effects of the isospin symmetry breaking on the charged $\Xi(1690)$ state in a similar manner to the neutral case due to the $K^-\Sigma^0$ - $\bar{K}^0\Sigma^-$ threshold difference.

5. Conclusion In this study we have investigated dynamics of $\bar{K}\Sigma$ and its coupled channels in the chiral unitary approach. It is a great advantage to employ the chiral unitary approach that a simple interaction kernel provided by the leading-order chiral perturbation theory does not contain free parameters and hence only the subtraction constants (or cut-offs) of the loop functions are the model parameters. The subtraction constants are fixed in the natural renormalization scheme, which can exclude explicit pole contributions from the loop functions, or by fitting the $\bar{K}^0\Lambda$ and $K^-\Sigma^+$ mass spectra to the experimental data.

As a result, we have found that, although the $\bar{K}\Sigma$ interaction from the leading-order chiral perturbation theory alone is slightly insufficient to bring a $\bar{K}\Sigma$ bound state, multiple scatterings in a meson-baryon coupled-channels approach can dynamically generate a $\bar{K}\Sigma$ quasibound state near the $\bar{K}\Sigma$ threshold. The obtained scattering amplitude can qualitatively reproduce the experimental data of the $\bar{K}^0\Lambda$ and $K^-\Sigma^+$ mass spectra and contains a Ξ^* pole as a $\bar{K}\Sigma$ molecule, which can be identified with the $\Xi(1690)$ resonance. Due to the small or vanishing couplings of the $\bar{K}\Sigma$ channel to others, we can naturally explain the decay properties of $\Xi(1690)$. We have also pointed out a possibility to observe effects of the isospin symmetry breaking on $\Xi(1690)$, such as the difference of the $K^-\Sigma^+$ and $\bar{K}^0\Sigma^0$ mass spectra, due to the difference of their thresholds when the $\Xi(1690)$ pole exists very close to the one of the $\bar{K}\Sigma$ thresholds.

Finally we suggest that further experimental studies on the $\Xi(1690)$ resonance and related $\bar{K}\Lambda$ and $\bar{K}\Sigma$ mass spectra are most welcome, since these experiments can constrain more the $\bar{K}\Sigma$ scattering

amplitude and the structure of the $\Xi(1690)$ resonance. Especially future studies on multi-strangeness systems at J-PARC, JLab, and other facilities can shed light on the structure of the $\Xi(1690)$ resonance. We also expect that high-statistics analyses on $\Xi(1690)$ by Belle, BaBar, and LHCb are promising. On the other hand, for the theoretical support in analyzing the $\Xi(1690)$ production, structure, and decay processes, we expect that we can utilize the same or a similar approach to the $\Lambda(1405)$ case, which has been extensively studied in the chiral unitary approach as well as in many other models, effective theories, and lattice QCD simulations. This is because both are dynamically generated resonances in the meson–baryon degrees of freedom and especially originate from the same flavor $SU(3)$ multiplet in the chiral unitary approach.

Acknowledgements

The author greatly acknowledges K. Imai for suggesting the author to study this topic and for useful discussions. The author also thanks Y. Kato for useful comments on Belle data and J. Nieves on the Ξ^* states in the chiral unitary approach. Stimulating discussions with A. Hosaka and his careful reading of the manuscript are gratefully acknowledged. This work is partly supported by the Grants-in-Aid for Young Scientists from JSPS (No. 15K17649) and for JSPS Fellows (No. 15J06538).

References

- [1] K. A. Olive *et al.* [Particle Data Group Collaboration], *Chin. Phys. C* **38**, 090001 (2014).
- [2] A. Bondar *et al.* [Belle Collaboration], *Phys. Rev. Lett.* **108**, 122001 (2012).
- [3] R. Aaij *et al.* [LHCb Collaboration], *Phys. Rev. Lett.* **115**, 072001 (2015).
- [4] C. Dionisi *et al.* [Amsterdam-CERN-Nijmegen-Oxford Collaboration], *Phys. Lett. B* **80**, 145 (1978).
- [5] S. F. Biagi *et al.*, *Z. Phys. C* **9**, 305 (1981).
- [6] S. F. Biagi *et al.*, *Z. Phys. C* **34**, 15 (1987).
- [7] M. I. Adamovich *et al.* [WA89 Collaboration], *Eur. Phys. J. C* **5**, 621 (1998).
- [8] K. Abe *et al.* [Belle Collaboration], *Phys. Lett. B* **524**, 33 (2002).
- [9] J. M. Link *et al.* [FOCUS Collaboration], *Phys. Lett. B* **624**, 22 (2005).
- [10] B. Aubert *et al.* [BaBar Collaboration], *Phys. Rev. D* **78**, 034008 (2008).
- [11] M. Ablikim *et al.* [BESIII Collaboration], *Phys. Rev. D* **91**, no. 9, 092006 (2015).
- [12] K. T. Chao, N. Isgur and G. Karl, *Phys. Rev. D* **23**, 155 (1981).
- [13] S. Capstick and N. Isgur, *Phys. Rev. D* **34**, 2809 (1986).
- [14] L. Y. Glozman and D. O. Riska, *Phys. Rept.* **268**, 263 (1996).
- [15] C. Garcia-Recio, M. F. M. Lutz and J. Nieves, *Phys. Lett. B* **582**, 49 (2004).
- [16] Y. Oh, *Phys. Rev. D* **75**, 074002 (2007).
- [17] M. Pervin and W. Roberts, *Phys. Rev. C* **77**, 025202 (2008).
- [18] D. Gamermann, C. Garcia-Recio, J. Nieves and L. L. Salcedo, *Phys. Rev. D* **84**, 056017 (2011).
- [19] N. Sharma, A. Martinez Torres, K. P. Khemchandani and H. Dahiya, *Eur. Phys. J. A* **49**, 11 (2013).
- [20] L. Y. Xiao and X. H. Zhong, *Phys. Rev. D* **87**, no. 9, 094002 (2013).
- [21] N. Kaiser, P. B. Siegel and W. Weise, *Nucl. Phys. A* **594**, 325 (1995).
- [22] E. Oset and A. Ramos, *Nucl. Phys. A* **635**, 99 (1998).
- [23] J. A. Oller and U. G. Meissner, *Phys. Lett. B* **500**, 263 (2001).
- [24] M. F. M. Lutz and E. E. Kolomeitsev, *Nucl. Phys. A* **700**, 193 (2002).
- [25] D. Jido, J. A. Oller, E. Oset, A. Ramos and U. G. Meissner, *Nucl. Phys. A* **725**, 181 (2003).
- [26] T. Hyodo and D. Jido, *Prog. Part. Nucl. Phys.* **67**, 55 (2012).
- [27] A. Ramos, E. Oset and C. Bennhold, *Phys. Rev. Lett.* **89**, 252001 (2002).
- [28] T. Sekihara, T. Hyodo and D. Jido, *Phys. Rev. C* **83**, 055202 (2011).
- [29] T. Hyodo, D. Jido and A. Hosaka, *Phys. Rev. C* **85**, 015201 (2012).
- [30] T. Hyodo, *Int. J. Mod. Phys. A* **28**, 1330045 (2013).
- [31] D. Gamermann, J. Nieves, E. Oset and E. Ruiz Arriola, *Phys. Rev. D* **81**, 014029 (2010).
- [32] J. Yamagata-Sekihara, J. Nieves and E. Oset, *Phys. Rev. D* **83**, 014003 (2011).
- [33] T. Sekihara, T. Hyodo and D. Jido, *PTEP* **2015**, no. 6, 063D04.
- [34] T. Hyodo, D. Jido and A. Hosaka, *Phys. Rev. C* **78**, 025203 (2008).
- [35] T. Hyodo, *Phys. Rev. C* **90**, no. 5, 055208 (2014).
- [36] C. Hanhart, J. R. Pelaez and G. Rios, *Phys. Lett. B* **739**, 375 (2014).
- [37] S. M. Flatte, *Phys. Lett. B* **63**, 224 (1976).
- [38] T. Hyodo and W. Weise, *Phys. Rev. C* **77**, 035204 (2008).